19

Protein Crystal Growth Under High Pressure

Yoshihisa Suzuki
Institute of Technology and Science,
The University of Tokushima,
Japan

1. Introduction

In this chapter, I would like to describe following two main roles of high pressure (up to 250 MPa) on protein crystal growth.

1. High pressure as a tool for enhancing crystallization of a protein
2. High pressure as a tool for modifying a three-dimensional (3D) structure of a protein molecule

For the first role, Visuri et al. reported that the total amount of obtained crystals of glucose isomerase (GI) was drastically increased with increasing pressure, for the first time (Visuri et al., 1990). Such drastic enhancements probably play an important role in increasing the success rate of 3D structure analysis of protein molecules, since crystallization is still the rate limiting step in the structure analysis process. Although they were the pioneers of this field, they did not do further studies on the growth mechanisms of GI crystals. After their pioneer work, many studies have been done on solubility (Section 2), nucleation (Section 3), and growth kinetics (Section 4) under high pressure. Here I would like to review and classify these studies, and present the potential of high pressure as a tool for enhancing protein crystallization.

For the second role, Kundrot & Richards were the pioneers of this field. They analyzed 3D structure of hen egg-white lysozyme under high pressure at the atomic level, for the first time (Kundrot & Richards, 1987). High-pressure protein crystallography is a prerequisite to understanding effects of pressure on an enzymatic activity of a protein at the atomic level (Makimoto et al., 1984). The structural information also plays an important role in the studies of deep-sea organisms (Yayanos, 1986). Pressure probably influences the protein structure through the structure of surrounding water molecules. Thus the protein structure under high pressure has to be solved with water of hydration at ambient temperatures, since a flash cooling method obviously influences the crystal structure (Charron et al., 2002); a freezing process of the method probably influences the structure of the surrounding water molecules, and the process prevents us from an "*in situ*" analysis of the protein structure with water of hydration. In addition, mainly due to the technical difficulties, total number of studies on high-pressure protein crystallography is not so many at this stage. In Section 5, I would like to review the studies on "*in situ*" protein structure analysis under high pressure, and present a new methodology for an ideal "*in situ*" structure analysis.

2. Solubility of protein crystals under high pressure

Solubility is generally important and indispensable to study an equilibrium state between a solution and crystal. Solubility is usually measured at the beginning of the crystallization research to determine the supersaturation σ ($\sigma = \ln(C/C_e)$, C: concentration of the solution, C_e: solubility), because the crystallization phenomena are often well described by using σ. Supersaturation is also named as the *driving force for crystallization*. For the studies at atmospheric pressure, σ has been useful for the discussion on the protein crystallization (Rosenberger et al., 1996). Thus, for a high-pressure study, the high-pressure σ is also useful to discuss the mechanisms of protein crystallization. To determine the high-pressure σ, the high-pressure solubility is indispensable.

2.1 Methodology

Many researchers have measured the solubility under high pressure. However, the solubility varies according to the method, even though the composition of the solution is almost the same (Suzuki et al., 2000b). The variation prevents us from the quantitative discussion. Therefore, the more sophisticated method is expected to measure the more accurate solubility. Here I would like to present several methods for the measurement of solubility under high pressure with their merits and demerits.

2.1.1 Change in the concentration of a supernatant solution with time (*ex situ*)

In general, this method is the most popular one for the solubility of crystals of small molecules. Groß et al. and Lorber et al. reported the solubility of tetragonal lysozyme crystals under high pressure by *ex situ* measurement (Groß & Jaenicke, 1991; Lorber et al., 1996). They incubated the supersaturated solution under high pressure for a certain period, then reduced the pressure and measured the concentration in the supernatant solution. They measured the solubility only from the supersaturated state, where the solubility is always uncertain from 0 $mgmL^{-1}$ to the asymptotic concentration. In addition, Suzuki et al. showed that an asymptotic concentration from a supersaturated state did not correspond to that from an undersaturated state in a realistic time scale (Suzuki et al., 2000b). Although this method provides concentration data directly, it takes very long time to attain an equilibrium condition.

2.1.2 Change in the concentration of a supernatant solution with time (*in situ*)

We have designed an *in situ* precise method of solubility measurement using a Mach-Zehnder interferometer (Suzuki et al., 1998) and measured *in situ* the solubility of lysozyme (Suzuki et al., 2000b). Using the method, the relative change in the concentration with time during equilibration was measured accurately and continuously starting from a supersaturated state (growth relaxation) and an undersaturated state (dissolution relaxation). The asymptotic concentration for the dissolution relaxation was regarded as the solubility. This method is more precise than *ex situ* one (described in 2.1.1). However, a long time period is still required to establish a solubility curve by this method, and this remains as one of the most serious barriers to further high-pressure studies.

2.1.3 Change in the crystal size with pressure

Takano et al. provided a much-improved technique based on in situ observation (Takano et al., 1997). They measured the equilibrium pressure in situ from supersaturation and

undersaturation. They gradually increased the pressure of the sample over a period of few days, and continuously recorded the images of the lysozyme crystal. The solubility was determined from changes in both the size of the crystal and the amount of the transmitted light through the crystal. Although they could shorten the period for one plot, a long time period was still required to establish a solubility curve.
We also measured the solubility of triclinic lysozyme crystals by observing the crystals before and after pressurization for two hours with high precision, although the measurements had been conducted *ex situ* (Suzuki et al., 2011).

2.1.4 Change in the concentration distribution around a crystal (*in situ*)

In order to decrease the time necessary for the solubility measurement under high pressure, another interferometric technique has been developed, which can determine the solubility of lysozyme within at most 3 hours (Sazaki et al., 1999). In the interferometric method, an equilibrium temperature of a given concentration is determined by observing the concentration distribution around a crystal. The distribution can be visualized by using a Michelson interferometer (Sazaki et al., 1999).
Under high pressure, the concentration distribution around the crystals was observed in situ with the Michelson interferometer. Figure 1 shows interferograms of the solution around a GI crystal under 100 MPa (Suzuki et al., 2002b). Here, the concentration of glucose isomerase was 35.4 $mgmL^{-1}$. If the temperature of the sample was set lower than its equilibrium temperature, the crystal grew (24.7 °C), and the fringes were bent in the vicinity of the crystal (Fig. 1(a)), because of the decrease in the concentration around the crystal. On the other hand, when the temperature was raised higher than its equilibrium temperature (44.1 °C), the crystal dissolved and the fringes bent in the opposite direction (Fig. 1(b)). From observation of the fringes around the crystal, we determined the equilibrium temperature of the crystal and solution of a given concentration.

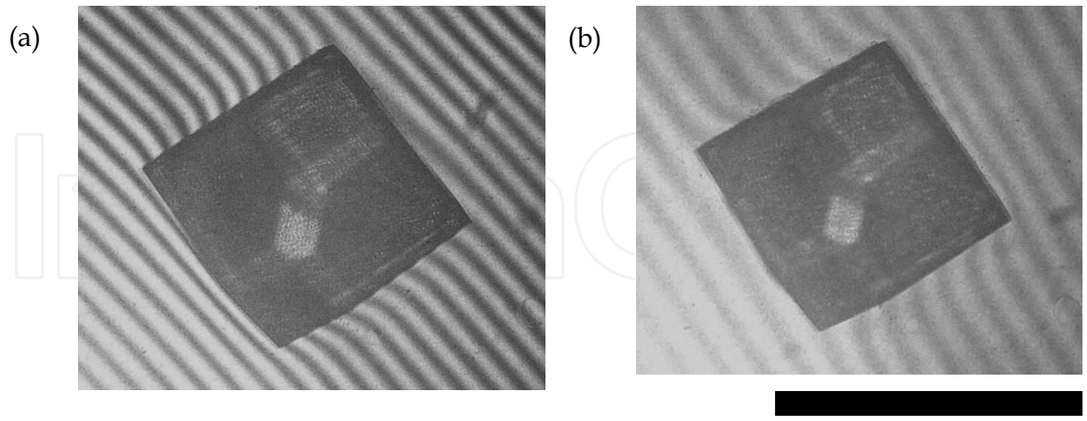

Fig. 1. Interferograms around the glucose isomerase crystal under 100 MPa (Suzuki et al., 2002b). Concentration of glucose isomerase in bulk solution is 35.4 $mgmL^{-1}$. (a) Growth (24.7 °C), (b) dissolution (44.1 °C). The scale bar represents 1 mm.

Although this technique reduced the measurement time for one data point drastically (within 3 hours), the error of the data points was generally larger than the method of 2.1.3.

2.1.5 Change in the position of steps or the morphology of ledges of crystals (*in situ*)

Among the many studies on protein solubilities so far, *in situ* observation of steps on crystal faces using a laser confocal microscope combined with a differential interference contrast microscope (LCM-DIM (Sazaki et al., 2004)) has been the most powerful method (step-observation method) for measuring the equilibrium temperatures T_e of protein crystals (Van Driessche et al., 2009; Fujiwara et al., 2010). Van Driessche et al. reported that this method yielded the highest precision in measurements of T_e of tetragonal hen egg-white lysozyme crystals (Van Driessche et al., 2009), and we found it produced the fastest results (Fujiwara et al., 2010). For high-pressure solubility, Fujiwara et al. measured that fastest and with highest precision, at this stage.

To tell the truth, we applied this method to measure high-pressure solubility of GI crystals for the first time (Suzuki et al., 2009, 2010a). In these papers, we also use the changes in the morphology of a ledge of a crystal, while the precision was not so high as that of the data measured by Fujiwara et al.

2.2 Solubility data

In addition to the above studies, many studies on the solubility of proteins under high pressure have been reported. The solubility, C_e, of tetragonal (Groß & Jaenicke, 2001; Lorber et al., 1996; Takano et al., 1997; Sazaki et al., 1999; Suzuki et al., 2000a, 2000b, 2002a; Kadri et al., 2002; Fujiwara et al., 2010) and monoclinic (Asai et al., 2004) hen lysozyme, turkey lysozyme (Kadri et al., 2002), and subtilisin (Webb et al., 1999; Waghmare et al., 2000a) crystal increased with increasing pressure, while that of orthorhombic hen lysozyme (Sazaki et al., 1999; Suzuki et al., 2002a), glucose isomerase (Suzuki et al, 2002b, 2005, 2009), and thaumatin (Kadri et al., 2002) crystal decreased with increasing pressure.

Protein crystals	Pressure dependence	Measurement time for one plot	Accuracy
Hen Lysozyme			
Tetragonal	↑ (Positive)	< 70 minutes (Fujiwara et al., 2010)	< ± 0.7 K in T_e
Orthorhombic	↓ (Negative)	< 3 hours (Sazaki et al., 1999)	< ± 4.8 K in T_e
Monoclinic	↑	< 6 hours (Asai et al, 2004)	< ± 0.4 mgmL^{-1} in C_e
Triclinic	↑	< 6 hours (Suzuki et al., 2011)	< ± 1.0 mgmL^{-1} in C_e
Turkey Lysozyme	↑	9 days (Kadri et al., 2002)	-
Purafect Subtilisin	↑	7 days (Webb et al., 1999)	-
Glucose Isomerase	↓	< 90 minutes (Suzuki et al., 2009)	< ± 2.5 K in T_e
Thaumatin	↓	9 days (Kadri et al., 2002)	-

Table 1. Effects of pressure on the solubility of proteins.

The above results are listed in Table 1. In general, the decrease in solubility with pressure results in the increase in nucleation rates and growth rates of crystals. From Table 1, three of eight crystals exhibit the decrease in solubility with pressure. Thus, application of high pressure to a protein solution would be useful for crystallizing previously uncrystallized proteins.

2.3 Thermodynamic analyses

From solubility data, thermodynamic parameters are often calculated using van't Hoff plots. If we assume that the effect of the activity coefficient is negligible, we can estimate the partial molar enthalpy of dissolution, ΔH, from Eq. (1) and the partial molar entropy of dissolution, ΔS, from Eq. (2).

$$\frac{\partial \ln C_e}{\partial (1/T)} = \frac{-\Delta H}{R}, \tag{1}$$

$$\frac{\partial RT \ln C_e}{\partial T} = \Delta S, \tag{2}$$

where C_e: solubility (mg mL^{-1}); R: gas constant.

To estimate ΔH lnC_e is plotted against T^{-1}. If we assume that ΔH does not depend on temperature, ΔH is estimated from the slope by linear fitting of the plot. In this section, weighted fitting was done, because the temperature error was large at lower concentration region. ΔS is estimated from T-RTlnC_e plots.

From the dependence of pressure on solubility, if we assume that the effect of the activity coefficient is negligible, the volume change accompanying the dissolution, ΔV ($\Delta V \equiv \bar{V} - V_c$, $\bar{V}$: the partial molar volume of the solute, V_c: molar volume of the crystal), is expressed as,

$$\Delta V = -RT\left[\frac{\partial \ln C_e}{\partial P}\right]_T. \tag{3}$$

If ΔV does not depend on pressure up to P MPa, the molar volume change accompanying the dissolution at 0.1 MPa is expressed as,

$$\Delta V = -RT\frac{\ln C_{e,P} - \ln C_{e,0.1}}{P\text{-}0.1}, \tag{4}$$

where $C_{e,P}$ and $C_{e,0.1}$ indicate the solubility at P MPa and 0.1 MPa, respectively.

All the above thermodynamic functions (ΔH, ΔS and ΔV) reported so far are listed in Table 2.

Negative value of ΔV indicates that the partial molar volume of a protein, $\bar{V}$, is smaller than the molar volume of a crystal, V_c, and *vice versa*. Figure 2 represents a simplified model of the states of the protein in the crystal and in solution.

Consider now the change from crystalline to the solution state. If we neglect any change in volume of the protein molecule, the bulk water, and the waters of hydration 2 (those around parts of the protein exposed in both crystal and solution), then ΔV is given by the volume of the waters of hydration 1 (around the contact surfaces of the protein) minus the volume occupied by these same water molecules as "free" water when the protein is in the crystalline state. For this volume change to be negative, as found for tetragonal lysozyme

crystals, the water molecules must be more tightly packed when hydrating the contact regions than when "free" in the bulk water. This, in fact, is expected to be the case for contacts containing a large number of hydrophilic residues. Correspondingly, the positive volume change on dissolution of glucose isomerase crystals implies that the contact surfaces tend to structure the waters of hydration such that they occupy a larger volume than in the bulk. It predicts that the contacts in glucose isomerase crystals should be more hydrophobic than in tetragonal lysozyme crystals.

Protein crystals	ΔV / cm^3mol^{-1}		ΔH / $kJmol^{-1}$		ΔS / $Jmol^{-1}K^{-1}$	
	0.1 MPa	Authors	0.1 MPa	100 MPa	0.1 MPa	100 MPa
Hen Lysozyme						
Tetragonal	-18±46	S&S	130±10	70±10	460±40	280±40
	-11.6	L				
	-5	We				
	-3.0±0.5	K				
Orthorhombic	5±18	S&S	35±3	35±5	140±10	140±20
Monoclinic		A	102±6	79±2		
Triclinic		S2011	113±4	97±4		
Turkey Lysozyme	-15±1	K				
Purafect Subtilisin	-21±1	We				
	-30±7	Wa				
Glucose Isomerase	54±31	S2002	160±40	210±60	420±100	580±180
Thaumatin	11±1	K				

Table 2. Thermodynamic functions of dissolution obtained by solubility data of protein crystals. Characters listed in Authors column indicate references as follows. S&S: (Sazaki et al., 1999; Suzuki et al., 2002a); L: (Lorber et al., 1996); We: (Webb et al., 1999); K: (Kadri et al., 2002); A: (Asai et al., 2004); S2011: (Suzuki et al., 2011); Wa: (Waghmare et al., 2000a); S2002: (Suzuki et al., 2002b).

The decrease in ΔS of tetragonal lysozyme crystal with pressure can be explained by a decrease in ΔV with pressure. Since the solution is more compressible than the crystal, the magnitude of ΔV is smaller under high pressure than under atmospheric pressure. Smaller $|\Delta V|$ under high pressure can lead to a smaller change in a degree of freedom. In the case of GI crystals, on the other hand, the increase in ΔS can be explained by the increase in ΔV with pressure. The change in ΔH is still not clear. Further crystallographic study on the hydration of the intermolecular contact regions or the other independent measurements of ΔV, ΔH and ΔS may explain these phenomena.

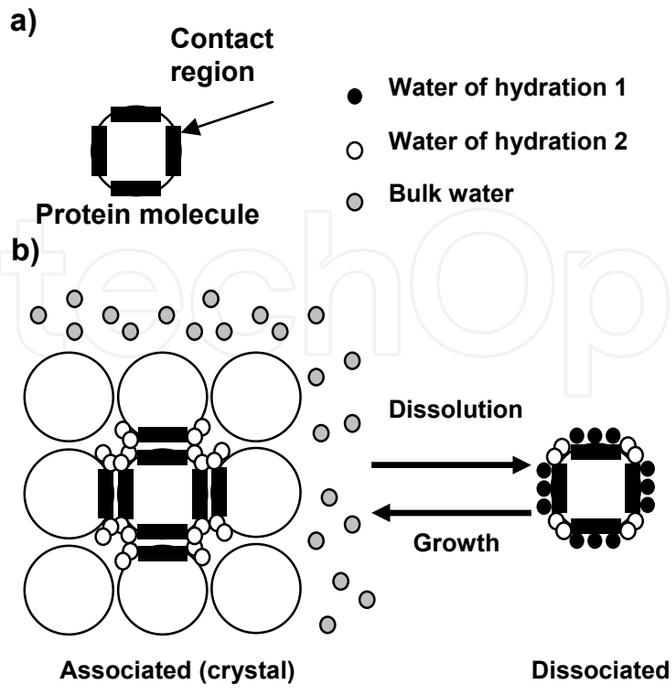

Fig. 2. Schematic diagrams of protein molecules in the crystal and solution (Suzuki et al., 2002a). In the crystal, the molecules are in contact with each other at the regions indicated in black. Hydrated water 1 and 2 represent water molecules hydrating the contact and non-contact regions of the protein, respectively. The volume change on dissolution is given mainly by the difference in volume between hydrated water 1 and bulk water.

3. Nucleation of protein crystals under high pressure

The mechanisms of high-pressure acceleration of 3D nucleation will play the most important role in the improvement of the success rate of crystallization, since the success rate of the 3D nucleation corresponds to that of the crystallization. The precise analyses of the supersaturation dependencies of 3D nucleation rate, J, will clarify the mechanisms.

Except for the data presented in our studies on GI crystals (Maruoka et al., 2010; Suzuki et al., 2010c), the effects of pressure on J have not been reported yet. Although Groß et al. discussed the effects of pressure on the nucleation kinetics using the Oosawa theory of protein self-assembly (Groß et al., 1993), and the group of Glatz discussed the activation volume of the nucleation using the number of crystals (Saikumar et al., 1998; Webb et al., 1999; Waghmare et al., 2000b; Pan & Glatz, 2002), neither group measured J under high pressure directly.

Thus, in this section, I would like to focus on our studies on GI crystals (Suzuki et al., 2009, 2010c; Maruoka et al., 2010).

3.1 Classical nucleation theory

The 3D nucleation rate (Volmer & Weber, 1926), J , is modified and expressed as follows (Suzuki et al., 1994):

$$J = \nu s n_t \exp(\frac{-\Delta G^*}{kT}), \tag{5}$$

where ν, s, n_t, ΔG^*, k, and T represent the collision rate of GI tetramers with critical nuclei, the sticking parameter for the addition of a GI tetramer to a critical nucleus, the number of GI tetramers in the unit volume of a solution, the Gibbs free energy for the formation of a critical nucleus of a GI crystal, the Boltzmann constant, and the absolute temperature, respectively. The variables s and ΔG^* can be expressed as follows (Boistelle & Lopez-Valero, 1990):

$$s = n \exp(\frac{-\varepsilon}{kT}), \tag{6}$$

and

$$\Delta G^* = \frac{f \Omega^2 \gamma^3}{(kT\sigma)^2}, \tag{7}$$

where n, ε, f, Ω and γ represent the total number of tetramers adjacent to the surface of a nucleus, the activation energy for the addition of a GI tetramer to a critical nucleus, the shape factor, the average volume occupied by a GI tetramer, and the surface free energy of the GI crystal, respectively. Substituting equation (6) and (7) for (5) and taking the natural log of both sides, we obtain the following expression:

$$\ln J = \ln(\nu n n t) - \frac{\varepsilon}{kT} - \frac{f \Omega^2 \gamma^3}{(kT)^3} \times \frac{1}{\sigma^2}. \tag{8}$$

3.2 Methodology

A high-pressure vessel with transparent sapphire windows was used (Maruoka et al., 2010; Suzuki et al., 2010c). An inner cell (inner volume = 1 × 6 × 20 mm^3) for *in situ* observation was made of glass slides, and equipped with soft silicone tubes for sample loading. The cell was set in the vessel, and crystals in the cell under high pressure were observed through the sapphire windows using a stereoscopic microscope (Nikon, SMZ800, objective: EDPlan×2 (N. A. = 0.2)). The solution and pressure medium were separated by soft silicone tubes of the cell. The solution around the crystals was pressurized *via* the tubes. The pressure in the vessel was well controlled automatically by a feedback system with a pressure sensor (accuracy of pressure: ± 0.5 MPa) and could be kept constant for a long time. The temperature of the cell was directly controlled using a Cu jacket with a Peltier element. We could control the temperature from 15.0 to 35.0 °C with the accuracy of ± 0.2 °C.

A supersaturated solution of a given GI concentration was transferred into an inner cell. The number of the observable crystals per unit volume N was counted with time t using a stereoscopic microscope. The nucleation rate J is defined as the slope of the tangent line of the t – N plots at the point of inflection. In practice, we fit Gompertz function, which is a sigmoid function, to the t – N plots, since Foubert et al. fit the Gompertz function to their data of released crystallization heat of fat crystals, and the fit of the Gompertz model seemed to be better than that of the mostly used Avrami model (Foubert et al., 2003). The Gompertz function we used is expressed as,

$$N = a\exp\{-\exp[-k(t - t_c)]\} \quad (9)$$

where t represents time, and a, k, and t_c are fitting parameters. We assume that J is defined as the slope of the tangent line of the Gompertz function at the point of inflection, since the slope provides the maximum value. From eq. (9), J is expressed as,

$$J = ak/e \quad (10)$$

Induction time τ is calculated by substituting $N = 1$ into eq. (9), and expressed as,

$$\tau = t_c - (1/k)\ln(-\ln(1/a)) \quad (11)$$

3.3 Three-dimensional nucleation rates

N increased with time in a sigmoidal-like fashion (Fig. 3). The Gompertz function fitted well all the t – N plots. From the fitting parameters and eq. (10), J was calculated and plotted against σ (Fig. 4). J increased with increasing pressure at the same σ. We also determined τ^{-1} using eq. (11). τ^{-1} also increased with increasing pressure at the same σ (Fig. 4). The increase in J and τ^{-1} with pressure at the same σ indicates that they are kinetically accelerated under high pressure.

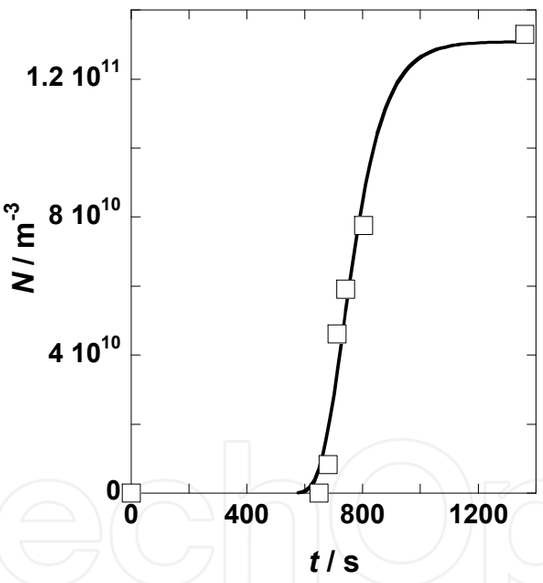

Fig. 3. Time course of the number of observed microcrystals at T = 20 °C, C = 27.07 mgmL^{-1}, and P = 100 MPa (Maruoka et al., 2010). Solid curve indicates a Gompertz function.

Although nucleation of protein crystals under high pressure has been already studied by a few researchers (Suzuki et al., 1994; Waghmare et al., 2000b; Pan & Glatz, 2002), no one has succeeded in measuring J directly and discussing the dependence of J on σ. We previously measured J of tetragonal lysozyme crystals under high pressure by *in situ* observation of the number of crystals using a diamond anvil cell (Suzuki et al., 1994). J decreased with increasing pressure at a constant concentration. However, since the solubility was not measured at that time, we could not separate the effects of solubility change under high pressure. Waghmare et al. and Pan et al. assumed that the final number of subtilisin crystals was proportional to J

(Waghmare et al., 2000b; Pan & Glatz, 2002), and they did not observe the transient number of the crystals. Thus, our results shown in Fig. 4 successfully clarified, for the first time, that the 3D nucleation of GI crystals was kinetically accelerated under high pressure.

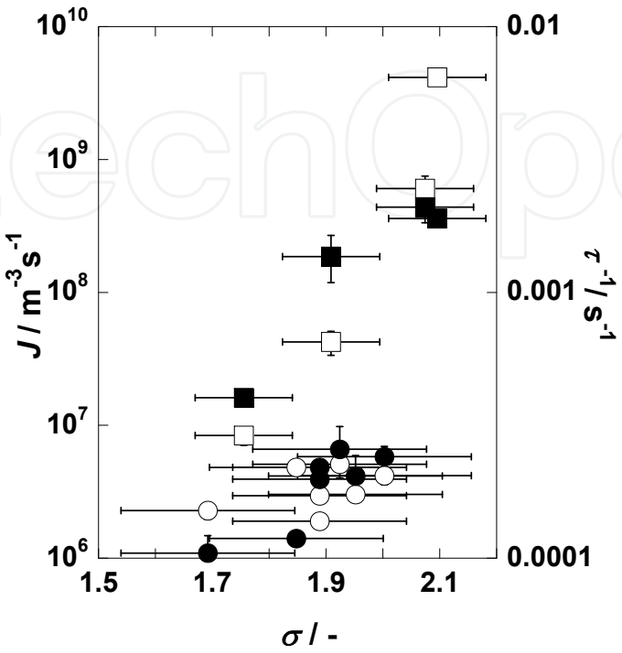

Fig. 4. J and τ^{-1} with supersaturation σ (Maruoka et al., 2010). Open and closed symbols indicate J and τ^{-1}, respectively. Circles and squares indicate the data measured under 0.1 and 100 MPa, respectively.

3.4 Kinetic analyses

We plotted the natural logarithm of J against $1 / \sigma^2$. ln$J$ increased with increasing pressure at the same value, $1 / \sigma^2$. Using eq. (10) and tentatively assuming that f equals 25 (Boistelle & Lopez-Valero, 1990), the average surface free energies γ at 20°C are calculated to be $(8 \pm 3) \times 10^{-5}$ and $(9 \pm 2) \times 10^{-5}$ Jm^{-2} at 0.10 and 100 MPa, respectively. γ does not change with pressure within experimental errors. This result does not correspond with our previous results, in which γ decreased with increasing pressure (Suzuki et al., 2005). This inconsistency is mainly due to the experimental errors in J. To confirm the pressure dependency of γ in detail, we will need to measure the two-dimensional (2D) nucleation rates with σ under high pressure (Suzuki et al., 2009, 2010a; Van Driessche et al., 2007).

On the other hand, the intercept of the linear fitting function shown in Fig. 2, $\ln(\nu n n_t) - \varepsilon / kT$, at 100 MPa is much larger than that at 0.10 MPa. This indicates that the activation energy for the addition of a GI tetramer to a critical nucleus, ε, decreases drastically with increasing pressure, since ν should not change so much, and n and n_t of 100 MPa are less than those of 0.10 MPa at the same σ.

3.5 Two-dimensional (2D) nucleation rates

We preliminarily measured *in situ* 2D nucleation rates J_s of 2D islands on the {011} face of glucose isomerase crystals at 0.1, 25 and 50 MPa. J_s increased with increasing pressure. For

these plots, GI concentration in the bulk solution C (= 5.6 mg mL^{-1}) and temperature (T = 26.4 °C) were constant throughout the measurement. Thus, the increases in J_s are completely due to the increase in pressure.

4. Growth kinetics of protein crystals under high pressure

To understand the mechanisms of crystal growth precisely, growth kinetics should be clarified. In this section, I would like to describe mainly following two topics.

1. Effects of high pressure on growth rates of crystal faces, R
2. Effects of high pressure on step velocities, V

4.1 Effects of high pressure on growth rates of crystal faces, *R*

Kinetic analyses of R provide useful information about growth mechanisms. Pressure effects on the kinetics of R of protein crystals are listed in Table 3.

Protein crystals	Pressure effects	Authors
Hen Lysozyme		
Tetragonal	Inhibition	Suzuki et al., 2000a
Orthorhombic	Inhibition	Nagatoshi et al., 2003
Monoclinic	Acceleration	Asai et al., 2004
Purafect Subtilisin	Inhibition	Waghmare et al., 2000a
Glucose Isomerase	Acceleration	Suzuki et al., 2005

Table 3. Effects of pressure on the growth kinetics of protein crystals.

4.1.1 Growth theory

How does pressure affects R kinetically? The following three hypotheses are conceivable. (1) An increasing pressure reduces the volume of the system, and thus elevates the protein concentration. (2) The rising pressure brings about changes in the crystals' growth mode. (3) Changes in growth parameters such as an activation energy, surface free energy, etc. occur with elevations in pressure.

(1) Elevation of the protein concentration through a reduction in the system volume

Let us first consider hypothesis (1). How much does the concentration change with increasing pressure? Kundrot & Richards reported that from 0.1 to 100 MPa the volume contraction of a tetragonal hen lysozyme (t-HEWL) crystal, the solvent in the crystal and the bulk solution were 1.1, 3.7 and 3.7 % (Kundrot & Richards, 1987, 1988), respectively. For a t-HEWL crystal, regardless of the increase in the protein concentration resulting from the volume contraction, the growth kinetics decelerates with increasing pressure (Suzuki et al., 2000a). In the case of the other protein crystals listed in Table 3, the volume contraction of the system is probably of the same order as that of the t-HEWL crystal (i. e. several percent). Thus, this hypothesis (1) can not explain the inhibition of the growth kinetics of protein crystals. In addition, it hardly explains the significant acceleration of the growth kinetics of monoclinic hen lysozyme and GI crystals.

(2) Changes in the crystals' growth mode

To evaluate the second hypothesis, we should first confirm the crystal growth mode under all the growth conditions. Since all the crystals described in this review had clear facets, the crystals formed via a layer-by-layer growth mechanism. Therefore, they must have grown in a spiral growth mode with screw dislocations or in a 2D nucleation growth mode (Fig. 5).

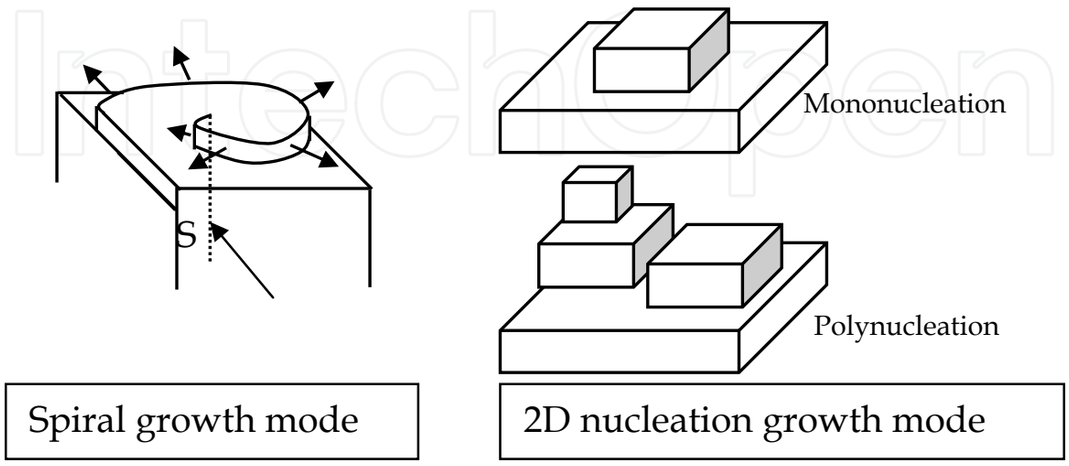

Fig. 5. Schematic illustrations of typical growth modes of crystals with clear faces.

If the density of the screw dislocations is sufficiently low, the growth rate R of the spiral growth mode is expressed as (Burton et al., 1951; Cabrera & Levine, 1956),

$$R = \frac{K_s h}{19 f_0 \kappa} \sigma^2 . \tag{12}$$

Here, K_s is a step kinetic coefficient, h a step height, f_0 the area which is occupied by a molecule on the crystal face, and κ a ledge free energy. In Table 3, only for t-HEWL and orthorhombic lysozyme (o-HEWL) and GI crystals, R of specific faces of the crystals were precisely measured. Supersaturation dependencies of R of the above three crystals were not fitted well using the equation (12).

Next, we take into account the 2D nucleation growth model. Actually, there are two models that can represent the 2D nucleation growth mode: one operating by mononucleation and the other by polynucleation. Through the following reasoning, we judged that the latter is the growth mode in the present cases. The growth rate in the mononucleation mode is proportional to the surface area of the relevant face (Markov, 1995). However, all R referred in the present review did not depend on the surface area, although different crystals of different size were used. In addition, to confirm the growth mode directly, we observed the surface topography *in situ* using a reflection type laser confocal microscope combined with a differential interference contrast microscope (LCM-DIM system) (Sazaki et al., 2004) for GI crystals. The 2D nucleation and subsequent lateral growth of the 2D islands were clearly observable. Thus, we concluded that the GI crystal grew in the polynucleation mode. In the case of t-HEWL, we also confirmed polynucleation growth under high pressure.

R in the polynucleation mode is expressed as (Suzuki et al., 2000a, 2005; Nagatoshi et al., 2003),

$$R = k_1 \exp(\frac{2\sigma}{3})(\exp\sigma - 1)^{2/3}\sigma^{1/6}\exp(\frac{-k_2}{\sigma}), \quad (13)$$

where k_1 and k_2 are expressed as,

$$k_1 = (\frac{\pi}{3})^{1/3} a^{13/3} h^{4/3} \nu \lambda_0^{-2/3} C_e^{4/3} \exp(-\frac{\varepsilon + \varepsilon_{ad} + 2\varepsilon_{kink}}{3kT}), \quad (14)$$

and

$$k_2 = \frac{\pi\gamma^2}{3k^2T^2}. \quad (15)$$

In Eqs. (13), (14) and (15), the following symbols are used: a is the distance between the molecules in the crystal; h is the step height; ν is the thermal frequency of a solute; λ_0 is the average distance between the kinks on a step; ε is the activation energy for a solute molecule to be incorporated into a critical nucleus; ε_{ad} is the activation energy for a solute molecule to be adsorbed on the crystal surface; ε_{kink} is the activation energy for a solute molecule to be incorporated into a kink site; γ is the molecular surface energy that represents the excess free energy due to unsatisfied bonds of a molecule at a step edge; and k is the Boltzmann constant. By nonlinear least squares fitting, eq. (13) reproduces the experimental data well. All experimental data were best fitted to the 2D nucleation growth mode of the polynucleation type. Hence we concluded that there was no change in the growth mode with increasing pressure. Thus pressure effects are mainly due to (3) Changes in growth parameters such as an activation energy, surface free energy, etc. with pressure.

4.1.2 Summary of kinetic analysis of *R*

For t-HEWL, o-HEWL, and GI crystals, R were measured with σ under high pressure. By fitting these data with the equation (13), kinetic constants k_1 and k_2 were calculated as shown in Table 4.

The value of k_1 of the {110} face of t-HEWL crystals at 100 MPA for the best fit ($k_1 = 7.1 \times 10^6$ nms^{-1}) is extraordinarily large and this value has less physical meaning. This is owing to the lack of data and error of R. As in eq. (14), there are too many factors to determine which dominate the increase in k_1 with pressure. Thus, I also showed the result in which I fixed k_1 value. The increase in k_1 and the decrease in k_2 result in the acceleration of growth kinetics. In Table 4, the dependence of k_1 and k_2 on pressure is generally complicated.

First, in the case of t-HEWL crystal, for both faces, k_1 increases with increasing pressure, while k_2 increases. This shows that the effect of the increase in surface free energy dominates the overall inhibition of the growth kinetics. Second, results of o-HEWL crystals show different pressure dependencies. Both k_1 and k_2 decrease with an increase of pressure. The decrease in k_1 dominates the inhibition of the growth kinetics under high pressure. Third, the acceleration of growth kinetics of GI crystals is mainly due to the decrease in surface free energy (k_2).

To study the effects of pressure on each parameter precisely, further accumulation of the data of R is needed.

Protein crystals and constants	Authors	Pressure / MPa		
		0.1	50	100
Hen Lysozyme				
Tetragonal	Suzuki et al., 2000a			
{110} face				
k_1 / nms^{-1}		0.84	3.5	7.1×10^6
k_2 / -		3.6	8.7	45
k_2 (k_1 = 0.84 nms^{-1} fixed) / -		3.6	5.4	9.6
{101} face				
k_1 / nms^{-1}		0.14	0.33	0.86
k_2 / -		1.0	3.8	6.5
k_2 (k_1 = 0.14 nms^{-1} fixed) / -		1.0	2.0	2.6
Orthorhombic	Nagatoshi et al., 2003			
k_1 / nms^{-1}		4.7 ± 1.3		1.7 ± 0.6
k_2 / -		2.0 ± 0.4		1.5 ± 0.5
Glucose Isomerase	Suzuki et al., 2005			
{101} face				
k_1 / nms^{-1}		7 ± 6		0.60 ± 0.08
k_2 / -		18 ± 2		3 ± 1

Table 4. Kinetic constants of 2D polynucleation growth.

4.2 Effects of high pressure on step velocities, *V*

In the case of a 2D nucleation growth model, since R is proportional to $J_s^{1/3}V^{2/3}$ (J_s: 2D nucleation rate, V: step velocity) (Markov, 1995), the model analyses of R are indirect and prevent further detailed analysis. *In situ* observation of the steps enables us to directly and separately measure J_s and V, which are necessary to elucidate the causes of high-pressure acceleration of the nucleation and growth. Hence, direct observation of individual elementary steps plays a crucial role in studies of crystallization under high pressure.

Direct observations of individual elementary steps on protein crystal surfaces have been carried out mainly by atomic force microscopy (AFM) (Durbin & Carlson, 1992; Durbin et al., 1993; McPherson et al., 2000). However, AFM does not work under high pressure (> 6 atm) at the present stage (Higgins et al., 1998). Besides, the scan of a cantilever would potentially affect the soft surfaces of protein crystals. Advanced optical microscopy is a promising alternative to directly and noninvasively observe individual elementary steps even under high pressure. Among various kinds of advanced optical microscopy, we adopted laser confocal optical microscopy combined with differential interference contrast microscopy (LCM-DIM), by which we have already succeeded in observing the elementary steps of GI crystals under atmospheric pressure (Suzuki et al., 2005). The development of a high-pressure vessel with an optical window thin enough to suppress optical aberration, also played a crucial role in the LCM-DIM system.

At this stage, V of GI crystals under high pressure are only available data (Suzuki et al, 2009, 2010a).

4.2.1 Theory of step velocities, *V*

Assuming a direct incorporation process, step velocity on a specific face of a GI crystal V is expressed as follows (Suzuki et al., 2009, 2010a):

$$V = \beta_{\text{step}}\Omega(C - C_e) \tag{16}$$

where β_{step} and Ω represent the step kinetic coefficient of the incorporation process of GI tetramers, which are the growth units of GI crystals, at kink sites on steps of GI crystals and the average volume occupied by a GI tetramer in the crystal, respectively. We used bulk concentration C instead of the concentration adjacent to a crystal surface, C_{surf}. β_{step} is expressed as follows (Chernov, 1984):

$$\beta_{step} = \nu \frac{p}{\lambda} a \exp(-\frac{\varepsilon_{kink}}{kT}), \tag{17}$$

where ν, p, λ, a, and $\varepsilon_{\text{kink}}$ represent the vibrational frequency of a GI tetramer, unit cell length parallel to a step, kink spacing, unit cell length perpendicular to the step, and activation energy of the incorporation of a GI tetramer into a kink site on the GI crystal surface, respectively. The variables ν, p, and a seldom change with increasing pressure. λ probably does not change with increasing pressure too much, since the shape of a step does not change with increasing pressure (Suzuki et al., 2009, 2010a). Most of the steps on GI crystal surfaces were straight ones and the shape of the steps did not change with increasing pressure. This means that λ did not change significantly; the change in β_{step} was mainly due to the change in $\varepsilon_{\text{kink}}$.

Based on the dependence of pressure on β_{step}, the volume change in going to the activation state in the incorporation process of GI molecules at the kink site on the step, $\Delta V^{\ddagger}$ ($\Delta V^{\ddagger} \equiv V^{\ddagger} - \bar{V}$, $V^{\ddagger}$: partial molar volume of the activated GI tetramer in the solution), is expressed as follows (Laidler, 1987):

$$\Delta V^{\ddagger} = -RT[\frac{\partial \ln \beta_{\text{step}}}{\partial P}]_T . \tag{18}$$

If $\Delta V^{\ddagger}$ does not depend on pressure up to P, $\Delta V^{\ddagger}$ at 0.10 MPa is expressed as follows:

$$\Delta V^{\ddagger} = -RT \frac{\ln \beta_{step,P} - \ln \beta_{step,0.10}}{P - 0.10}, \tag{19}$$

where $\beta_{\text{step},P}$ and $\beta_{\text{step},0.10}$ indicate the step kinetic coefficients at P and 0.10 MPa, respectively.

4.2.2 Experimental

This study made use of an LCM-DIM system (Olympus Optical Co., Ltd.). To measure V of GI crystals precisely, a super-luminescent diode (SLD) laser (Amonics Ltd., model ASLD68-050-B-FA: λ = 680 nm), whose coherence length is about 10 μm, was adopted as a light source.

Figure 6 shows a schematic illustration of a high-pressure vessel and a GI crystal. A high-pressure vessel with a 1-mm-thick sapphire window (Syn-corporation, Ltd., PC-100-MS) was specially designed and used for the *in situ* observation of crystal surfaces under high pressure. We used an O-ring to provide a seal between the sapphire window and a stainless steel support. The surface of the support attached to the sapphire window was processed by mirror polishing to increase the pressure that the O-ring could withstand. In this study, achieving a balance in the thickness of the sapphire window was particularly important, since a thinner window decreases optical aberration, while a thicker one raises the withstand pressure. To our knowledge, the vessel used in this study provides top performance in *in situ* observation of crystal surfaces. The volume of sample space in this vessel is 8.3 mm^3 (4.3 mm in height and 1.6 mm in diameter).

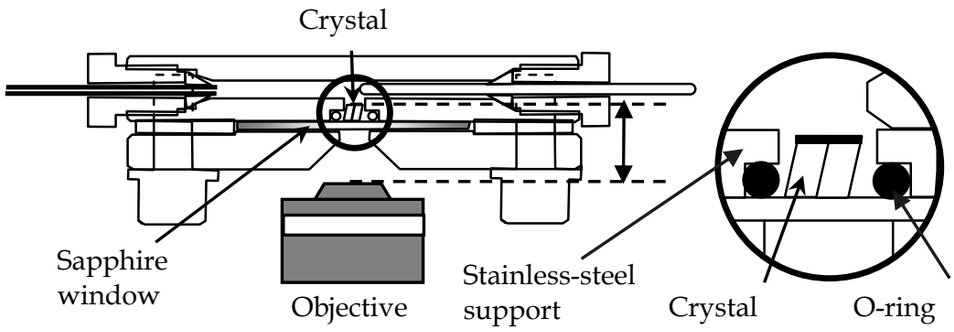

Fig. 6. Schematic illustration of an experimental setup.

To compensate for the optical aberration caused by the light transmitted through the sapphire window, an objective with a compensation ring for a cover glass with a thickness of 0 – 2 mm (Olympus Optical Co., Ltd., SLCPlanFl 40X) also played an important role. Precise adjustments of the compensation ring of the objective and the shear amount of the Nomarski prism were indispensable for obtaining a high contrast level of elementary steps.

For *in situ* observation of elementary steps under high pressure, seed crystals were placed directly on the sapphire window of the high-pressure vessel to minimize the optical aberration. The seed crystals were prepared as follows. A suspension of GI crystals (Hampton Research Co., Ltd., HR7-100), containing 0.91 M ammonium sulfate and 1 mM magnesium sulfate in 6 mM tris hydrochloride buffer (pH = 7.0) (Tris-HCl is known as the most insensitive buffer to pressure) (Neuman et al., 1973), was dissolved (~ 33 mg mL^{-1}) and filtered (Suzuki et al., 2002b). Then the filtrate was transferred onto the sapphire window and sealed with an o-ring and a glass slide.

After a few small crystals appeared on the window at 10 °C, the crystals were grown at room temperature (~ 22 °C) until they reached an appropriate size for the observation (typically ≥ 100 μm). The crystals placed on the window were rinsed with a GI solution of 5.6 mg mL^{-1}, and then the window with the crystals was fitted into the high-pressure vessel filled with a GI solution of 5.6 mg mL^{-1}. In this study we prepared ≤ 10 crystals (size ~ 150 μm) in the 1.6 mmφ O-ring on the sapphire window. Thus, the average separation between the crystals was ~ 300 μm.

4.2.3 Step velocities

Step velocities V on the {011} faces at 0.1 and 50 MPa were measured in the range of protein concentrations C = 5.3 – 8.9 mg mL^{-1}. As shown in Figure 7(a), V increased with increasing pressure. The increase in V is attributed to both kinetic and thermodynamic contributions as shown in eq. (16).

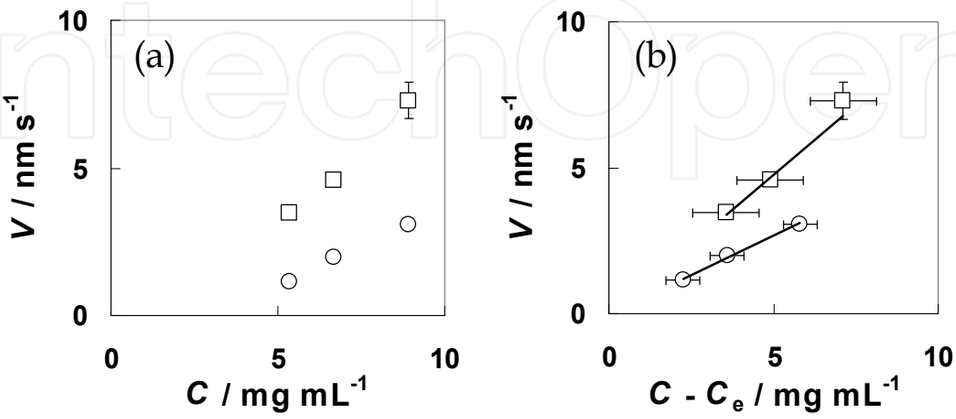

Fig. 7. Step velocities V on the {011} faces of GI crystals as a function of C (a) and C – C_e (b) (Suzuki et al., 2009, 2010a). V was measured at 0.1 MPa (○) and 50 MPa (□). Temperature was 25.0 °C. The lines shown in (b) indicate the results of weighed linear fitting.

To separate the kinetic contribution (β_{step}) from the thermodynamic one (C – C_e), we replotted V as a function of C - C_e (Figure 7 (b)). The slopes of the straight lines shown in Figure 7 (b) correspond to $\beta_{step}\Omega$ in eq. (16) at 0.1 and 50 MPa. We have measured Ω under 100 MPa by X-ray crystallography, and found that Ω decreased by only 1.1% with increasing pressure: Ω were (4.79 ± 0.03) × 10^{-25} and (4.74 ± 0.08) × 10^{-25} m^3 at 0.1 and 100 MPa, respectively (Tsukamoto, 2009). Thus, we concluded that β_{step} increased with increasing pressure kinetically. β_{step} thus obtained were (3.2 ± 0.2) × 10^{-7} and (5.7 ± 0.9) × 10^{-7} m s^{-1} at 0.1 and 50 MPa (here we assume that Ω at 50 MPa is same as that at 0.1 MPa), respectively. From these data, we calculated $\Delta V^{\ddagger}$ to be –28 ± 8 cm^{3}mol^{-1} using equation (19).

C_e values at 25°C (2.6 ± 1.4) and (0.8 ± 0.4) mgmL^{-1} at 0.10 and 50 MPa, respectively (Suzuki et al., 2009, 2010a). From these data, we calculated ΔV to be -60 ± 40 cm^{3}mol^{-1} using equation (4). The absolute value of $\Delta V^{\ddagger}$ is almost half that of ΔV.

Such volumetric parameters are strongly related to the dehydration process during the incorporation of a growth unit into a kink site. Thus, further data accumulation will be useful for understanding the dehydration process, which should be one of the most important mechanisms of protein crystallization.

5. X-ray crystallography of protein crystals under high pressure

From the viewpoint of "in situ" high-pressure protein crystallography at the atomic level, five reports have been published so far (Kundrot & Richards, 1987; Urayama et al., 2002; Collins et al., 2005, 2007; Colloc'h et al., 2006). Kundrot et al. reported a three-dimensional structure of a protein (lysozyme) molecule under 100 MPa for the first time (Kundrot &

Richards, 1987). They used a Beryllium (Be) vessel with a stainless steel capillary tube. They revealed anisotropic contraction of the molecule and the increase in the number of ordered water in the crystal with increasing pressure. Urayama et al. and Collins et al. also used Be vessels (Urayama et al., 2002; Collins et al., 2005, 2007). Colloc'h et al. used a diamond anvil cell (DAC), and they could collect 2.3 Å resolution data of urate oxidase (Colloc'h et al., 2006).

However, each method has some problems. All the Be vessels equipped capillary tubes, and the tubes were obstacles to the free rotation of the vessels on goniometers during data collection processes. In the case of a DAC, the accuracy of pressure measurements with ruby fluorescence is low, although the DAC can generate much higher pressures than the Be vessels can do. The error of the pressure measurements in a DAC is usually larger than 10 MPa. In addition, there are usually geometrical constraints on data collection processes with a DAC.

A stand-alone type Be vessel solves all the above problems. Without connecting to the capillary tube, the vessel can freely rotate. With a simple free-piston type pressure indicator, we can monitor pressure in the vessel. In this section, I would like to present our most recent work on high-pressure x-ray protein crystallography.

5.1 Methodology

A stand-alone type high-pressure Be vessel (Syn-corporation Ltd.) was constructed for "in situ" high-pressure protein crystallography at the atomic level (Suzuki et al., 2010b). The vessel equips a Be tube, a stainless steel base, a pressure valve, a coupler joint and a free-piston type pressure indicator. The pressure indicator was composed of a free piston and two springs, and pressure was monitored within ± 1 MPa. From calibration plots of the indicator, we obtained the following equation.

$$h = (0.46 \pm 0.05) + (0.0983 \pm 0.0009)\, P. \tag{20}$$

Here h is the displacement of the piston in mm, and P shows pressure in MPa. The Be tube contains 1% BeO, which reduces X-ray transmittance, and this BeO content is less than that in Urayama's Be tube (2.5%) (Urayama et al., 2002). The thickness of the tube wall is 1.08 mm, and it is also less than that of Kundrot's tube (2.25 mm) (Kundrot & Richards, 1987).

5.2 High pressure X-ray analyses of crystals grown at ambient pressure

Glucose isomerase from *Streptomyces rubiginosus* (Hampton Research, HR7-100) was used without further purification. A GI crystal (~ 0.5 mm) was prepared at atmospheric pressure on the inner wall of a glass capillary (Hampton Research, HR6-164) with its growing solution. The solution contains 0.91 M ammonium sulfate, 1 mM magnesium sulfate, and these are dissolved in 6 mM tris hydrochloride buffer (pH = 7.0). The details of the preparation of the crystal are as follows. First, smaller seed crystals were prepared as described elsewhere (Suzuki et al, 2002b). Second, one of the smaller seed crystals was transferred into a growth solution (the GI concentration of the solution was 28 $mgmL^{-1}$) in a glass capillary. Third, the seed crystal was incubated for 3 days at 26 °C. Last, the capillary with the crystal and solution was transferred into our high-pressure vessel without replacing the solution. We did not remove the solution, since hydrostatic pressure should be transmitted *via* the solution. A diffraction data set was collected at room temperature on an imaging-plate detector (Rigaku Co., R-AXIS VII) using a rotating copper-anode in-house

generator operating at 40 kV and 20 mA (0.8 kW). Such a relatively mild condition is suitable for "in situ" structure analyses, since a high-intensity X-ray radiation easily increases the temperature of a crystal and water molecules around the crystal; the crystal easily dissolves and deteriorates.

Rotation diffraction spots of a GI crystal and powder diffraction rings of a Be tube are shown in Fig. 8. The data were processed using Crystal Clear (Rigaku Corporation, Tokyo).

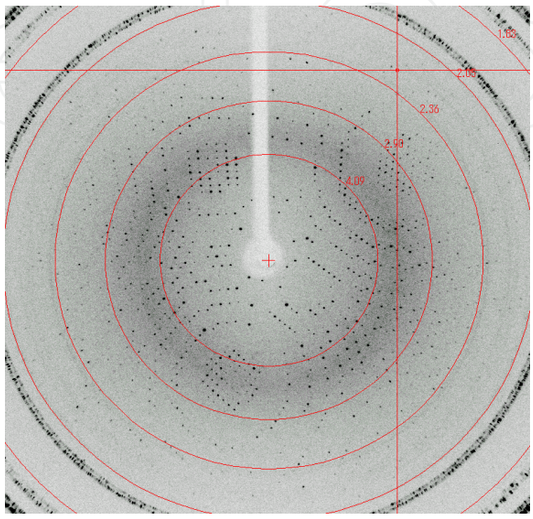

Fig. 8. Rotation diffraction spots of a GI crystal and diffraction rings of a polycrystalline Be tube (Suzuki et al., 2010b).

We successfully collected a 2.0 Å resolution data set of a GI crystal. Pressure could be kept constant at 100 ± 1 MPa for > 24 hours in stand-alone conditions (without connecting to a pressure generator). Although the crystal dissolved a little after the data collection process (> 3 hours irradiation with X-rays), we confirmed that this vessel is sufficiently useful for "in situ" high-pressure protein crystallography.

Strictly speaking, no one has done true "in situ" high-pressure protein crystallography, and a direct result has not been achieved yet. Kundrot et al., Urayama et al., Collins et al., and Colloc'h et al. prepared their crystals at atmospheric pressure, and then pressurized and analyzed the crystals. In such cases, proteins in a crystal shrink with keeping their bonding structure in the crystal during the pressurization. Thus, the pressurized structure in the crystal can be different from that in a solution. In contrast, Charron et al. prepared thaumatin crystals under high pressure, and analyzed the crystals at 100 K after depressurization (Charron et al., 2002). The 3D molecular structures of thaumatin in the depressurized crystals were essentially same as those of unpressurized control crystals. The result suggested that the crystal lattice of thaumatin is elastic. Our group analyzed depressurized, pressurized, and unpressurized GI crystals (Tsukamoto, 2009). A GI structure of the depressurized crystal was essentially same as that of thee unpressurized crystal. Only a GI structure of the pressurized crystal shrinked a little under 100 MPa. This result seems to support Charron's conclusion. However, all the above results are indirect.

To achieve direct results, we should collect a high-resolution, "in situ", and high-pressure data set of a crystal that has nucleated and grown under high pressure. Our setup will achieve the direct results. We can incubate a sufficiently supersaturated protein solution in

our vessel under a pressure as long as possible with connecting to a pressure-generating apparatus. After the appropriate nucleation and sufficient growth of crystals from the solution, we can separate the vessel from the capillary tube and directly collect a high-resolution diffraction data set of the crystals with keeping the pressure in the vessel constant.

6. Conclusions

In this chapter, I have presented the great potentialities of high pressure for the promotion of studies on the fundamental growth mechanisms of protein crystals and correlation between the function and 3D structures of protein molecules. Key points in this review are described shortly as follows.

1. As a tool for enhancing the crystal growth, three of eight proteins show the decrease in its solubility under high pressure. Application of high pressure during the screening processes would be useful because of such high probability.
2. Acceleration of growth and nucleation kinetics of glucose isomerase crystals occurred under high pressure.
3. Step velocities under high pressure provided us direct information on activation volume. Activation volume was negative in the case of glucose isomerase crystals. Precise discussion on the activation volume will be useful for understanding dehydration mechanisms during an incorporation process of a protein molecule into a kink site.
4. Usefulness of our standalone-type Be vessel for high-pressure protein crystallography was confirmed. With the vessel, precise high-pressure 3D structure analysis of protein crystals which are also grown under high pressure.

7. Acknowledgments

In this chapter, our studies were supported mainly by two research and education programs and two grants. Studies on solubility, nucleation rates, face growth rates, and step velocities under high pressure were partially supported by "Program for an improvement of education" promoted by the University of Tokushima, the inter-university cooperative research program of the Institute for Materials Research, Tohoku University, and Grants-in Aid (Nos. 16760014 and 19760009 (Y.S.)) for Scientific Research from the Ministry of Education, Culture, Sports, Science and Technology of Japan.

8. References

Asai, T., Suzuki, Y., Sazaki, G., Tamura, K., Sawada, T., & Nakajima, K. (2004). Effects of High Pressure on the Solubility and Growth Kinetics of Monoclinic Lysozyme Crystals. *Cellular and Molecular Biology*, Vol. 50, No. 4, (June 2004), pp. 329-334, ISSN 0145-5680

Boistelle, R., & Lopez-Valero, I. (1990). Growth Units and Nucleation: the Case of Calcium Phosphates. *Journal of Crystal Growth*, Vol. 102, No. 3, (May 1990), pp. 609-617, ISSN 0022-0248

Burton, W.K., Cabrera, N., & Frank, F.C. (1951). The Growth of Crystals and the Equilibrium Structure of Their Surfaces. Philosophical Transactions of the Royal Society of London A., Vol. 243, No. 866, (June 1951), pp. 299-358, ISSN 1471-2962

Cabrera, N., & Levine, M.M. (1956). On the Dislocation Theory of Evaporation of Crystals. *Philosophical Magazine*, Vol. 1, No. 5, (May 1956), pp. 450-458, ISSN 0031-8086

Charron, C., Robert, M.-C., Capelle, B., Kadri, A., Jenner, G., Giegé, R., & Lorber, B. (2002). X-ray Diffraction Properties of Protein Crystals Prepared in Agarose Gel under Hydrostatic Pressure. *Journal of Crystal Growth*, Vol. 245, No. 3-4, (November 2002), pp. 321-333, ISSN 0022-0248

Chernov, A.A. (1984). *Modern Crystallography III Crystal Growth*, Springer-Verlag, ISBN 3-540-11516-1, Berlin Heidelberg New York Tokyo

Collins, M.D., Hummer, G., Quillin, M.L., Matthews, B.W., & Gruner, S.M. (2005). Cooperative Water Filling of a Nonpolar Protein Cavity Observed by High-Pressure Crystallography and Simulation. *Proceedings of the National Academy of Sciences of the United States of America*, Vol. 102, No. 46, (November 2005), pp. 16668-16671, ISSN 0027-8424

Collins, M.D., Quillin, M.L., Hummer, G., Matthews, B.W., & Gruner, S.M. (2007). Structural Rigidity of a Large Cavity-Containing Protein Revealed by High-Pressure Crystallography. *Journal of Molecular Biology*, Vol. 367, No.3, (March 2007), pp. 752-763, ISSN 0022-2836

Colloc'h, N., Girard, E., Dhaussy, A.-C., Kahn, R., Ascone, I., Mezouar, M., & Fourme, R. (2006). High Pressure Macromolecular Crystallography: the 140-MPa Crystal Structure at 2.3 Å Resolution of Urate Oxidase, a 135-kDa Tetrameric Assembly. *Biochimica et Biophysica Acta*, Vol. 1764 (2006), No. 3, (March 2006), pp 391-397, ISSN 1570-9639

Durbin, S.D., & Carlson, W.E. (1992). Lysozyme Crystal Growth Studied by Atomic Force Microscopy. *Journal of Crystal Growth*, Vol. 122, No. 1-4, (August 1992), pp. 71-79, ISSN 0022-0248

Durbin, S.D., Carlson, W.E., & Saros, M.T. (1993). In Situ Studies of Protein Crystal Growth by Atomic Force Microscopy. *Journal of Physics D: Applied Physics*, Vol. 26, No. 8B, (August 1993), pp. B128-B132, ISSN 0022-3727

Foubert, I., Dewettinck, K., & Vanrolleghem, P.A. (2003). Modelling of the Crystallization Kinetics of Fats. *Trends in Food Science & Technology*, Vol. 14, No. 3, (March 2003), pp. 79-92, ISSN 0924-2244

Fujiwara, T., Suzuki, Y., Sazaki, G., & Tamura, K. (2010). Solubility Measurements of Protein Crystals under High Pressure by *In Situ* Observation of Steps on Crystal Surfaces. *Journal of Physics: Conference Series*, Vol. 215, (March 2010), pp. 012159-1-5, ISSN 1742-6588

Groß, M., & Jaenicke, R. (1991). Growth Inhibition of Lysozyme Crystals at High Hydrostatic Pressure. *FEBS Letters*, Vol. 284, No. 1, (June 1991), pp. 87-90, ISSN 0014-5793

Groß, M., & Jaenicke, R. (1993). A Kinetic Model Explaining the Effects of Hydrostatic Pressure on Nucleation and Growth of Lysozyme Crystals. *Biophysical Chemistry*, Vol. 45, No. 3, (January 1993), pp. 245-252, ISSN 0301-4622

Higgins, S.R., Eggleston, C.M., Knauss, K.G., Boro, C.O. (1998). A Hydrothermal Atomic Force Microscope for Imaging in Aqueous Solution up to 150 °C. *Review of Scientific Instruments*, Vol. 69, No. 8, (August 1998), pp. 2994-2998, ISSN 0034-6748

Kadri, A., Lorber, B., Jenner, G., & Giegé, R. (2002). Effects of Pressure on the Crystallization and the Solubility of Proteins in Agarose Gel. *Journal of Crystal Growth*, Vol. 245, No. 1-2, (November 2002), pp. 109-120, ISSN 0022-0248

Kundrot, C.E., & Richards, F.M. (1987). Crystal Structure of Hen Egg-White Lysozyme at a Hydrostatic Pressure of 1000 Atmospheres. *Journal of Molecular Biology*, Vol. 193, No. 1, (January 1987), pp. 157-170, ISSN 0022-2836

Kundrot, C.E., & Richards, F.M. (1988). Effect of Hydrostatic Pressure on the Solvent in Crystals of Hen Egg-White Lysozyme. *Journal of Molecular Biology*, Vol. 200, No. 2, (March 1988), pp. 401-410, ISSN 0022-2836

Laidler, K.J. (1987). *Chemical Kinetics, 3rd ed.*, Harper & Row, ISBN 0060438622, New York, USA

Lorber, B., Jenner, G., & Giegé, R. (1996). Effect of High Hydrostatic Pressure on Nucleation and Growth of Protein Crystals. *Journal of Crystal Growth*, Vol. 158, No. 1-2, (January 1996), pp. 103-117, ISSN 0022-0248

Makimoto, S., Suzuki, K., & Taniguchi, Y. (1984). Pressure Dependence of the a-Chymotrypsion-Catalyzed Hydrolysis of Amide and Anilides. Evidence for the single-proton-transfer mechanism. *The Journal of Physical Chemistry*, Vol. 88, No. 24, (November 1984), pp. 6021-6024, ISSN 0022-3654

Markov, I.V. (1995). *Crystal Growth for Beginners : Fundamentals of Nucleation, Crystal Growth, and Epitaxy,* World Scientific, ISBN 9810215312, Singapore, Singapore

Maruoka, T., Suzuki, Y., & Tamura, K. (2010). Effects of High Pressure on the Three-Dimensional Nucleation Rates of Glucose Isomerase Crystals. *Journal of Physics: Conference Series*, Vol. 215, (March 2010), pp. 012158-1-5, ISSN 1742-6588

McPherson, A., Malkin, A.J., Kuznetsov, Y.G. (2000). Atomic Force Microscopy in the Study of Macromolecular Crystal Growth. Annual Review of Biophysics and Biomolecular Structure, Vol. 29, pp. 361-410, ISSN 1056-8700

Nagatoshi, Y., Sazaki, G., Suzuki, Y., Miyashita, S., Matsui, T., Ujihara, T., Fujiwara, K., Usami, N., & Nakajima, K. (2003). Effects of High Pressure on the Growth Kinetics of Orthorhombic Lysozyme Crystals. *Journal of Crystal Growth*, Vol. 254, No. 1-2, (June 2003), pp 188-195, ISSN 0022-0248

Neuman, R.C., Jr., Kauzmann, W., & Zipp, A. (1973). *The Journal of Physical Chemistry*, Vol. 77, No. 22, (October 1973), pp. 2687-2691, ISSN 0022-3654

Pan, X., & Glatz, C.E. (2002). Solvent Role in Protein Crystallization as Determined by Pressure Dependence of Nucleation Rate and Solubility. *Crystal Growth & Design*, Vol. 2, No. 1, (January 2002), pp. 45-50, ISSN 1528-7483

Rosenberger, F., Vekilov, P.G., Muschol, M., & Thomas, B.R. (1996). Nucleation and Crystallization of Globular Proteins – What We Know and What is Missing. *Journal of Crystal Growth*, Vol. 168, No. 1-4, (October 1996), pp. 1-27, ISSN 0022-0248

Saikumar, M.V., Glatz, C.E., & Larson, M.A. (1998). Lysozyme Crystal Growth and Nucleation Kinetics. *Journal of Crystal Growth*, Vol. 187, No. 2, (May 1998), pp. 277-288, ISSN 0022-0248

Sazaki, G., Matsui, T., Tsukamoto, K., Usami, N., Ujihara, T., Fujiwara, K., & Nakajima, K. (2004). In Situ Observation of Elementary Growth Steps on the Surface of Protein Crystals by Laser Confocal Microscopy. *Journal of Crystal Growth*, Vol. 262, No. 1-4, (February 2004), pp. 536-542, ISSN 0022-0248

Sazaki, G., Nagatoshi, Y., Suzuki, Y., Durbin, S.D., Miyashita, S., Nakada, T., & Komatsu, H. (1999). Solubility of Tetragonal and Orthorhombic Lysozyme Crystals under High Pressure. *Journal of Crystal Growth*, Vol. 196, No. 2-4, (January 1999), pp. 204-209, ISSN 0022-0248

Suzuki, Y., Miyashita, S., Komatsu, H., Sato, K., & Yagi, T. (1994). Crystal Growth of Hen Egg White Lysozyme under High Pressure. Japanese Journal of Applied Physics, Vol. 33, No. 11A, (November 1994), pp. L1568-L1570, ISSN 0021-4922

Suzuki, Y., Sawada, T., Miyashita, S., Komatsu, H. (1998). *In Situ* Measurements of the Solubility of Crystals under High Pressure by an Interferometric Method. *Review of Scientific Instruments*, Vol. 69, No. 7, (July 1998), pp. 2720-2724, ISSN 0034-6748

Suzuki, Y., Miyashita, S., Sazaki, G., Nakada, T., Sawada, T., & Komatsu, H. (2000a). Effects of Pressure on Growth Kinetics of Tetragonal Lysozyme Crystals. *Journal of Crystal Growth*, Vol. 208, No. 1-4, (January 2000), pp. 638-644, ISSN 0022-0248

Suzuki, Y., Sawada, T., Miyashita, S., Komatsu, H., Sazaki, G., & Nakada, T. (2000b). An Interferometric Study of the Solubility of Lysozyme Crystals under High Pressure. *Journal of Crystal Growth*, Vol. 209, No. 4, (February 2000), pp. 1018-1022, ISSN 0022-0248

Suzuki, Y., Sazaki, G., Miyashita, S., Sawada, T., Tamura, K., & Komatsu, H. (2002a). Protein Crystallization under High Pressure. *Biochimica et Biophysica Acta*, Vol. 1595, No. 1-2, (March 2002), pp. 345-356, ISSN 0167-4838

Suzuki, Y., Sazaki, G., Visuri, K., Tamura, K., Nakajima, K., & Yanagiya, S. (2002b). Significant Decrease in the Solubility of Glucose Isomerase Crystals under High Pressure. *Crystal Growth & Design*, Vol. 2, No. 5, (September 2002), pp 321-324, ISSN 1528-7483

Suzuki, Y., Sazaki, G., Matsui, T., Nakajima, K., & Tamura, K. (2005). High-Pressure Acceleration of the Growth Kinetics of Glucose Isomerase Crystals. *The Journal of Physical Chemistry B*, Vol. 109, No. 8, (March 2005), pp. 3222-3226, ISSN 1089-5647

Suzuki, Y., Sazaki, G., Matsumoto, M., Nagasawa, M., Nakajima, K., & Tamura, K. (2009). First Direct Observation of Elementary Steps on the Surfaces of Glucose Isomerase Crystals under High Pressure. *Crystal Growth & Design*, Vol. 9, No. 10, (October 2009), pp. 4289-4295, ISSN 1528-7483

Suzuki, Y., Sazaki, G., Matsumoto, M., Nagasawa, M., Nakajima, K., & Tamura, K. (2010a). First Direct Observation of Elementary Steps on the Surfaces of Glucose Isomerase Crystals under High Pressure (Additions and Corrections). *Crystal Growth & Design*, Vol. 10, No. 4, (April 2010), pp. 2020-2020, ISSN 1528-7483

Suzuki, Y., Tsukamoto, M., Sakuraba, H., Matsumoto, M., Nagasawa, M., & Tamura, K. (2010b). Design of a standalone-type beryllium vessel for high-pressure protein crystallography. *Review of Scientific Instruments*, Vol. 81, No. 8, (August 2010), pp. 084302-1-3, ISSN 0034-6748

Suzuki, Y., Maruoka, T., & Tamura, K. (2010c). Activation Volume of Crystallization and Effects of Pressure on the Three-Dimensional Nucleation Rate of Glucose Isomerase. *High Pressure Research*, Vol. 30, No. 4, (December 2010), pp. 483-489, ISSN 0895-7959

Suzuki, Y., Konda, E., Hondoh, H., & Tamura, K. (2011). Effects of Temperature, Pressure, and pH on the Solubility of Triclinic Lysozyme Crystals. *Journal of Crystal Growth*, Vol. 318, No. 1, (March 2011), pp. 1085-1088, ISSN 0022-0248

Takano, K.J., Harigae, H., Kawamura, Y. & Ataka, M. (1997). Effect of Hydrostatic Pressure on the Crystallization of Lysozyme Based on In Situ Observations. *Journal of Crystal Growth*, Vol. 171, No. 3-4, (February 1997), pp. 554-558, ISSN 0022-0248

Tsukamoto, M. (2009). *Master Thesis*, Graduate School of Advanced Technology and Science, The University of Tokushima

Urayama, P., Phillips, Jr., G.N., & Gruner, S.M. (2002). Probing Substrates in Sperm Whale Myoglobin Using High-Pressure Crystallography. *Structure*, Vol. 10, No. 1, (January 2002), pp. 51-60, ISSN 0969-2126

Van Driessche, A.E.S., Sazaki, G., Otalora, F., Gonzalez-Rico, F.M., Dold, P., Tsukamoto, K., & Nakajima, K. (2007). Direct and Noninvasive Observation of Two-Dimensional Nucleation Behavior of Protein Crystals by Advanced Optical Microscopy. *Crystal Growth & Design*, Vol. 7, No. 7, (September 2007), pp. 1980-1987, ISSN 1528-7483

Van Driessche, A.E.S., Gavira, J.A., Patiño Lopez, L.D., & Otalora, F. (2009). Precise Protein Solubility Determination by Laser Confocal Differential Interference Contrast Microscopy. *Journal of Crystal Growth*, Vol. 311, No. 13, (June 2009), pp. 3479-3484, ISSN 0022-0248

Visuri, K., Kaipainen, E., Kivimaki, J., Niemi, H., Leisola, M., & Palosaari, S. (1990). A New Method for Protein Crystallization Using High Pressure. *Bio/Technology*, Vol. 8, No. 6, (June 1990), pp. 547-549, ISSN 0733-222X

Volmer, M., & Weber, A. (1926). Keimbildung in Übersättigten Gebilden. *Zeitschrift für Physikalische Chemie*, Vol. 199, pp. 277-301, ISSN 0044-3336

Waghmare, R.Y., Webb, J.N., Randolph, T.W., Larson, M.A., & Glatz, C.E. (2000a). Pressure Dependence of Subtilisin Crystallization Kinetics. *Journal of Crystal Growth*, Vol. 208, No. 1-4, (January 2000), pp. 678-686, ISSN 0022-0248

Waghmare, R.Y., Pan, X.J., & Glatz, C.E. (2000b). Pressure and Concentration Dependence of Nucleation Kinetics for Crystallization of Subtilisin. *Journal of Crystal Growth*, Vol. 210, No. 4, (March 2000), pp. 746-752, ISSN 0022-0248

Webb, J.N., Waghmare, R.Y., Carpenter, J.F., Glatz, C.E., & Randolph, T.W. (1999). Pressure Effect on Subtilisin Crystallization and Solubility, *Journal of Crystal Growth*, Vol. 205, No. 4, (September 1999), pp. 563-574, ISSN 0022-0248

Yayanos, A.A. (1986). Evolutional and Ecological Implications of the Properties of Deep-Sea Barophilic Bacteria. *Proceedings of the National Academy of Sciences of the United States of America*, Vol. 83, No. 24, (December 1986), pp. 9542-9546, ISSN 0027-8424

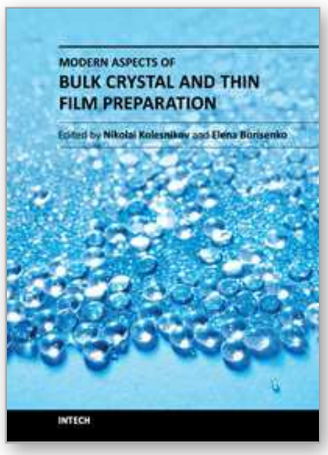

Modern Aspects of Bulk Crystal and Thin Film Preparation

Edited by Dr. Nikolai Kolesnikov

ISBN 978-953-307-610-2
Hard cover, 608 pages
Publisher InTech
Published online 13, January, 2012
Published in print edition January, 2012

In modern research and development, materials manufacturing crystal growth is known as a way to solve a wide range of technological tasks in the fabrication of materials with preset properties. This book allows a reader to gain insight into selected aspects of the field, including growth of bulk inorganic crystals, preparation of thin films, low-dimensional structures, crystallization of proteins, and other organic compounds.

How to reference

In order to correctly reference this scholarly work, feel free to copy and paste the following:

Yoshihisa Suzuki (2012). Protein Crystal Growth Under High Pressure, Modern Aspects of Bulk Crystal and Thin Film Preparation, Dr. Nikolai Kolesnikov (Ed.), ISBN: 978-953-307-610-2, InTech, Available from: http://www.intechopen.com/books/modern-aspects-of-bulk-crystal-and-thin-film-preparation/protein-crystal-growth-under-high-pressure

INTECH
open science | open minds

InTech Europe
University Campus STeP Ri
Slavka Krautzeka 83/A
51000 Rijeka, Croatia
Phone: +385 (51) 770 447
Fax: +385 (51) 686 166
www.intechopen.com

InTech China
Unit 405, Office Block, Hotel Equatorial Shanghai
No.65, Yan An Road (West), Shanghai, 200040, China
中国上海市延安西路65号上海国际贵都大饭店办公楼405单元
Phone: +86-21-62489820
Fax: +86-21-62489821

IntechOpen